On-off optical switching of the magnetic and structural properties in a spin-crossover complex

On-off optical switching of the magnetic and structural properties in a spin-crossover complex

K. Kato and M. Takata
RIKEN SPring-8 Center, 1-1-1 Kouto, Sayo-cho, Sayo-gun, Hyogo 679-5198, Japan

Y. Moritomo[a)]
Department of Physics, University of Tsukuba, Tsukuba 305-8571, Japan

A. Nakamoto and N. Kojima
Graduate School of Arts and Sciences, University of Tokyo, Tokyo 153-8902, Japan

A photoexcitation is one of the promising external fields to control the material phases. Here, the authors have demonstrated that the magnetic and structural properties of a spin-crossover complex, $Fe(phen)_2(NCS)_2$ (phen=1,10-phenanthroline), can be reversibly switched by the on-off action of the continuous photoexcitation at the same temperature. The structural data suggest that the density of the high-spin Fe^{2+} in the photoinduced phase is about 0.88. Suppressed atomic vibrations of the photoinduced phase exclude the conventional heating effect as the origin for the observed optical switching. © *2007 American Institute of Physics.* [DOI: 10.1063/1.2736213]

The photoexcitation is one of the most promising methods to reversibly control the material phase/property of organic and metal-organic compounds, which may be utilized as an optical switching device. Among the materials, iron(II) spin-crossover complexes[1–8] is one of the most interesting systems, as they are known to show the photoinduced low-spin (LS) to high-spin (HS) transition. However, this light-induced excited spin state trapping[1] (LIESST) is a long-festering phenomenon, and we need a troublesome thermal annealing and/or another photoexcitation to restore the material. This is a serious limitation for the development of optical switching device based on the spin-crossover complexes. In this letter, we report on a fast on-off optical switching of the magnetic and structural properties of $Fe(phen)_2(NCS)_2$ (phen=1,10-phenanthroline) at the same temperature by a single continuous-wave laser at 532 nm. There exists a threshold excitation light intensity I_{th} for the on-off optical switching phenomenon, suggesting that some cooperative interaction among the photoinduced HS species plays a crucial role.

The spin-crossover complex, $Fe(phen)_2(NCS)_2$, consists of the neutral $Fe(phen)_2(NCS)_2$ molecules within the orthorhombic ($Pbcn$;$Z=4$) cell.[9] In the $Fe(phen)_2(NCS)_2$ molecule, the iron(II) is surrounded by four N atoms belonging to 1,10-phenanthrolines and two N atoms of $(NCS)^-$ groups. The synthesis procedure of $Fe(phen)_2(NCS)_2$ was described elsewhere.[9] The compound shows a thermally induced phase transition from the LS phase to the HS phase at $T_C=176$ K. The thermally induced phase transition is accompanied by a volume expansion, reflecting the elongation of the Fe–N bond distances by 0.10–0.20 Å. At low temperature ($T<60$ K), the compound shows the LIESST phenomenon[10] by the photoirradiation of a He/Ne laser (633 nm).

Figure 1(a) shows an example of the on-off optical switching of $Fe(phen)_2(NCS)_2$ at 100 K, where no LIESST phenomenon is observed. The vertical axis is the density of the high-spin species (n_{HS}). The magnitude of n_{HS} is esti-

mated by the magnetic susceptibility measured in a Quantum Design magnetic properties measuring system (MPMS) superconducting quantum interference device magnetometer operated at 1000 Oe. The n_{HS} value shows a clear binary response to the on-off action of the continuous-wave laser irradiation at 532 nm. The transition speed is about 10 s. Hereafter, we will call the phase under photoirradiation as "on phase." In this phase, the creation process of the HS species overwhelms the thermal relaxation process of them. In Fig. 1(b), we plotted the n_{HS} value in the on phase against the excitation powder (I). The n_{HS} value begins to increase when I reaches a threshold value ($I_{th}=6$ mW/mm^2), and then reaches around 0.8 at $I=20$ mW/mm^2. Such a threshold behavior is absent in the conventional LIESST phenomenon. Désaix *et al.*[11] reported a similar threshold behavior, but with much slower transition time of order of hour, in a mixed crystal $Fe_{0.5}Co_{0.5}(btr)_2(NSC)_2H_2O$. They attributed the behavior to the cooperative effect of the relaxation. In order to explain much faster switching time as observed in this letter, however, we need an additional cooperative effect in the creation process of the HS species. We think that the internal pressure[6] induced by the photoinduced HS species, whose
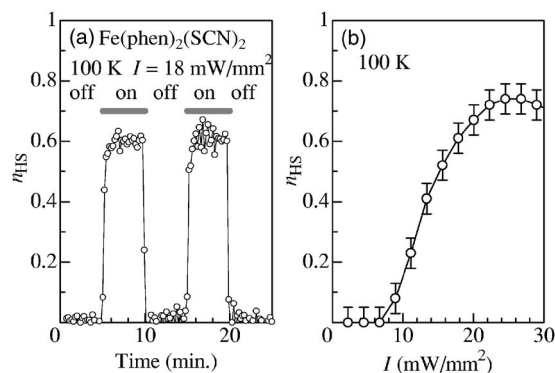

FIG. 1. (a) On-off optical switching of the density of the high-spin species (n_{HS}) measured at 100 K. The gray horizontal bar represents the on-off action of the excitation light at 532 nm. (b) Excitation power density (I) dependence of n_H in the "on phase" at 100 K.
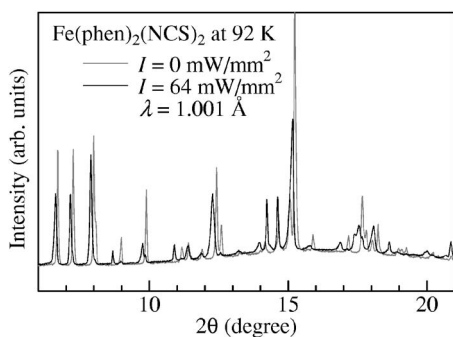
[a)]Electronic mail: moritomo@sakura.cc.tsukuba.ac.jp

FIG. 2. X-ray powder diffraction patterns of $Fe(phen)_2(NCS)_2$ at 92 K under photoexcitation ($I=64$ mW/mm^2: black curve) and without photoexcitation (gray curve).

FIG. 3. (a) Cell volume (V) of $Fe(phen)_2(NCS)_2$ at 92 K against excitation power density (I). Closed and open circles stand for the LS phase and the on phase, respectively. (b) Mass fraction (s) of the on phase against I. A broken straight line is merely the guide for the eyes.

ionic radius ($=0.74$ Å) is much larger than that ($=0.61$ Å) of the LS Fe^{2+}, causes a structural phase transition into the HS-rich phase. This argument is further supported by the fact that the cell volume of the photoinduced phase is much larger than that of the LS phase (*vide infra*).

In order to reveal the structural feature of the on phase, we have performed a synchrotron-radiation x-ray powder diffraction measurement at the SPring-8 BL02B2 beamline.[12] A 532 nm laser beam was weakly focused onto the capillary with a convex lens ($f=20$ cm); the laser spot size (about 2 mm) is larger than the x-ray beam size (1×0.5 mm^2). The reflections were collected on an imaging plate, installed in a large Debye-Scherrer camera. The reflections were collected on an imaging plate in the 2θ range of $3°–76°$. Figure 2 shows a part of the powder diffraction pattern at 92 K: black (gray) curve represents the patterns with (without) photoexcitation. Even though the photoexcitation considerably changes the powder diffraction patterns, the pattern change is reversible for a repeated on-off action of the laser irradiation. The sample under photoexcitation is stable for more than 11 h, without any deterioration of the diffraction pattern. The gray curve without photoexcitation is well reproduced by the Rietveld refinement with the single orthorhombic ($Pbcn$; $Z=4$) phase, that is, the LS phase. On the other hand, we need an additional photoinduced phase to reproduce the black curve. The space group of the photoinduced phase is found to be the same as that of the LS phase. We ascribe the additional phase to the on phase, as observed in Fig. 1(a). Here, we emphasize that the formation of the photoinduced phase cannot be ascribed to the conventional thermal heating effects. Because the degree of the thermal atomic vibrations of the photoinduced phase, which was estimated by the so-called Wilson plot,[13] is nearly the same as that at 92 K and is much smaller than that at 260 K.

Figure 3(a) shows the cell volume (V) of the LS phase (filled circles) and the photoinduced phase (open circles) against I. The V value of both the phases shows negligible change against I. The cell volume ($V=2.28$ nm^3) of the photoinduced phase is about 4% larger than that ($=2.20$ nm^3) of the LS phase, reflecting the larger ionic radius of the HS Fe^{2+}. In Fig. 3(b), we plotted the mass fraction (s) of the photoinduced phase. As shown by the eye-guided broken line, the formation of the photoinduced phase shows the threshold behavior, consistently with the magnetic behavior [see Fig. 1(b)].

Here, let us compare the microscopic structure of the on phase with the other HS phases, that is, the low-temperature
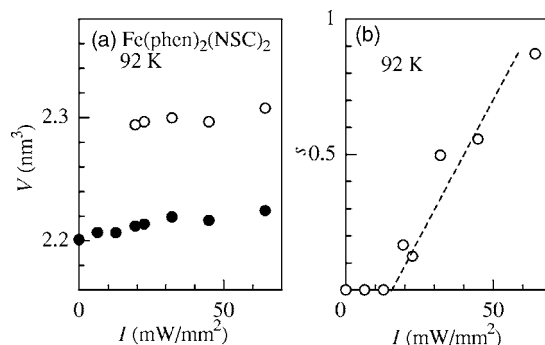
LIESST phase and the thermally induced HS phase. We listed in Table I the geometrical features of the FeN_6 octahedron of $Fe(phen)_2(NCS)_2$ molecule. The FeN_6 octahedron in the HS phase has larger distortion (Σ) and larger volume (v) as compared with those of the LS phase. At the bottom of Table I, we listed the relative volume (v/V) of the FeN_6 octahedron normalized by the cell volume. In spite of the 3% thermal shrinkage, the magnitude of v/V ($=0.006\,35$) in the LIESST phase at 30 K (Marchivie *et al.*[10]) is nearly the same as that ($=0.006\,39$) at 260 K. This is probably because the LIESST phase is a metastable HS phase, which can be produced also by the thermal quenching. Here, we emphasize that the magnitude of v/V ($=0.006\,22$) in the on phase is smaller than the other HS phases. If we postulate a linear relation between n_{HS} and v/V, n_{HS} of the on phase is estimated to be about 0.88. Such a suppressed n_{HS} value should be ascribed to the dynamical nature of the on phase, where the creation process of the HS species balances with the thermal relaxation process of them.

Finally, let us investigate the charge density distribution of the $Fe(phen)_2(NCS)_2$ molecule. Figures 4(b)–4(d) show the isodensity surface contours (0.45 e Å^{-3}) of the molecule determined by the maximum entropy method (MEM) Rietveld analysis[14–17] on the x-ray powder diffraction patterns. The isodensity surface contour is sharp at 92 K [the LS phase: Fig. 4(b)] and in the on phase [Fig. 4(c)], while it is

TABLE I. Geometry of the FeN_6 octahedron of $Fe(phen)_2(NCS)_2$. d_{Fe-N_i} ($i=1$, 2, and 3) is the $Fe-N_i$ bond distance. Σ is defined by the sum of the absolute values of the deviation from 90° of the 12 *cis* angles of the FeN_6 octahedron. V and v are the cell volume and the volume of the FeN_6 octahedron, respectively. These values were determined by the Rietveld analysis of the x-ray powder diffraction patterns. N_1 and N_2 atoms are located on 1,10-phenanthroline, while N_3 are on NCS^- ion.

| | HS phase | | | LS phase |
	30 K[a] LIESST	92 K on phase	260 K	92 K
d_{Fe-N_1} (Å)	2.177	2.197(3)	2.218(1)	2.006(2)
d_{Fe-N_2} (Å)	2.184	2.197(5)	2.218(2)	1.976(3)
d_{Fe-N_3} (Å)	2.006	2.046(5)	2.071(4)	1.930(4)
Σ(degree)	64	64	64	38
V (Å^3)	2242	2308	2319	2199
v (Å^3)	14.24	14.35	14.82	11.32
v/V	0.006 35	0.006 22	0.006 39	0.005 15

[a]Reference 10.
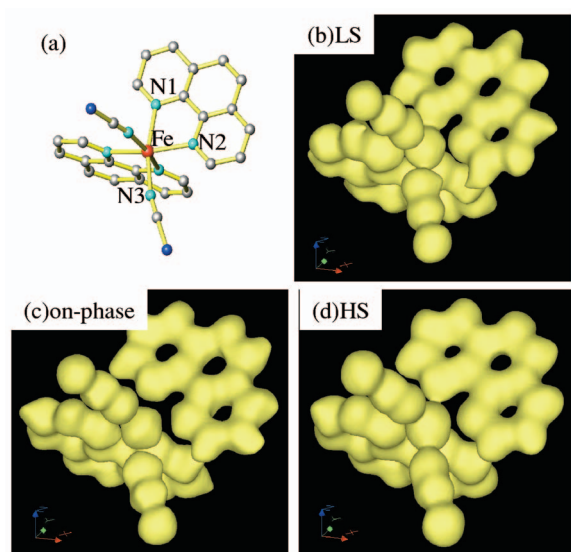
FIG. 4. (Color) (a) Ball and stick picture of the Fe(phen)$_2$(NCS)$_2$ molecule. Isodensity surface contour (0.45 Å^{-3}) of the Fe(phen)$_2$(NCS)$_2$ molecule in (b) the LS phase at 92 K, (c) the on phase at 92 K, and (d) the HS phase at 260 K, determined by the MEM/Rietveld analysis.

rather blurred at 260 K [the thermally induced HS phase: Fig. 4(d)]. This again indicates that the degree of the thermal atomic vibrations of the photoinduced phase is nearly the same as that at 92 K. Here, we emphasize that the respective Fe(phen)$_2$(NCS)$_2$ molecule in the photoinduced phase repeats the photoexcitation and thermal relaxation processes. The iron ion of the on phase [Fig. 4(c)] is more isolated as compared with the LS phase [Fig. 4(b)], reflecting the longer Fe–N bond distance.

In conclusion, we demonstrated the on-off optical control of the magnetic and structural properties of a molecular solid. The photoinduced phase, in which the creation process of the HS species balances with the thermal relaxation process of them, exists only under photoexcitation. Based on the structural analysis, we concluded that the photoinduced phase is a *cold* phase with suppressed HS density and long-range periodicity. Thus, the photoexcitation is a promising external field to control the material phase, especially when it is coupled with material parameters such as the spin state or the internal pressure.

[1] A. Hauser, J. Jeftić, H. Romstedt R. Hinek, and H. Spiering, Coord. Chem. Rev. **190**, 471 (1999).
[2] Y. Ogawa, S. Koshihara, K. Koshino, T. Ogawa, C. Urano, and H. Takagi, Phys. Rev. Lett. **84**, 3181 (2000).
[3] T. Tayagaki and K. Tanaka, Phys. Rev. Lett. **86**, 2886 (2001).
[4] N. O. Moussa, G. Molnár, S. Bonhommeau, A. Zwick, S. Mouri, K. Tanaka, J. A. Real, and A. Bousseksou, Phys. Rev. Lett. **94**, 107205 (2005).
[5] X. J. Liu, Y. Moritomo, T. Kawamoto, A. Nakamoto, and N. Kojima, J. Phys. Soc. Jpn **72**, 1615 (2003).
[6] Y. Moritomo, M. Kamiya, A. Nakamura, A. Nakamoto, and N. Kojima, Phys. Rev. B **73**, 012103 (2006).
[7] H. Liu, A. Fujishima, and O. Sato, Appl. Phys. Lett. **86**, 122511 (2005).
[8] S. Bonhommeau, G. Molnár, A. Galet, A. Zwick, J. A. Real, J. J. McGarvey, and A. Bousseksou, Angew. Chem., Int. Ed. **44**, 4069 (2005).
[9] B. Gallois, J. A. Real, C. Hauw, and J. Zarembowich, Inorg. Chem. **29**, 1152 (1990).
[10] M. Marchivie, P. Guionneau, J. A. K. Howard, G. Chastanet, J. F. Létard, A. E. Goeta, and D. Chasseau, J. Am. Chem. Soc. **124**, 194 (2002).
[11] A. Désaix, O. Roubeau, J. Jeftic, J. G. Haasnoot, K. Boukheddaden, E. Codjovi, J. Linarés, M. Nogués, and F. Varret, Eur. Phys. J. B **1998**, 183.
[12] E. Nishibori, M. Takata, K. Kato, M. Sakata, Y. Kubota, S. Aoyagi, Y. Kuroiwa, M. Yamakawa, and N. Ikeda, Nucl. Instrum. & Methods 467-468, 1045 (2001).
[13] See EPAPS Document No. E-APPLAB-90-077718 for magnitude of the thermal atomic vibrations estimated by the Wilson plot. This document can be reached via a direct link in the online's HTML reference section or via the EPAPS nomepage (http://www.aip.org/pubserves/epaps.html).
[14] M. Takata, E. Nishibori, and M. Sakata, Z. Kristallogr Z. Kristallogr. **216**, 71 (2001).
[15] M. Takata and M. Sakata, Acta Crystallogr., Sect. A: Found. Crystallogr. **52**, 287 (1996).
[16] H. Tanaka, M. Takata, E. Nishibori, K. Kato, T. Ishii, and M. Sakata, J. Appl. Crystallogr. **35**, 282 (2002).
[17] The diffraction data were collected for 11 h at 92 K (the LS phase and the on phase), 260 K (the HS phase). The number of the structural factors derived by the Rietveld analysis was 672, 700, and 706 for the LS phase, the on phase, and the thermally induced HS phase, respectively. The maximum (minimum) d values were 8.6 (1.2), 8.7 (1.2), and 8.7 A (1.2 A) for the off state, the on state, and the HS phases. The MEM analyses were carried out with a program ENIGMA (Ref. 16) using $132 \times 100 \times 172$ pixels. The R_F factors based on the MEM charge densities are 3.5%, 2.7%, and 4.3% for the LS phase, the on phase, and the HS phase, respectively.